Projection of Diffracted Optical Atom Traps

By

Jeremy Kruger

Advisor, Dr. Glen Gillen

Department of Physics, California Polytechnic University SLO

September 28, 2011

Approval Page

Title: Projection of Diffracted Optical Atom Traps

Author: Jeremy Kruger

Date Submitted: June 3, 2011

Senior Project Advisor: Dr. Glen Gillen

_____

Signature

_____

Date

Contents

1 Abstract **8**

2 Introduction **8**

3 Theory **9**

3.1 RDT and BDT Traps 9

3.2 Determining a Model 10

3.3 Propagation Through Lens 11

3.4 Projection into MOT 13

4 Experimental Setups **13**

4.1 Imaging Setups 13

4.1.1 Equipment List 14

4.2 Glass Vacuum Chamber Setup and Implementation of the Cage System 15

4.2.1 Equipment List 15

5 Results **16**

5.1 Calculation and Computational Results 16

5.2 Experimental Results 17

5.3 Projections to Determine Effects of Glass Vacuum Chamber Tube 18

6 Discussion **19**

7 Conclusions **19**

A 40 mm Lens Images **24**

B 100 mm Lens Images **32**

List of Tables

1 Acronyms and Symbols 7

2 Primary RDT and Primary BDT Trap Images 17

List of Figures

1 Plot of the intensity distribution along the z-axis of a 780-nm laser beam incident upon a circular aperture with radius 25-μm. The relative intensities are normalized and are depicted by colors ranging from the red-detuned traps with the highest intensity and the blue-detuned traps with the lowest intensity [5]. 11
2 Theoretical setup for near-field diffraction patterns to an vacuum chamber holding a MOT cloud of cold atoms. 14
3 Experimental setup for finding RDT and BDT traps. 15
4 Experimental setup using a cage system and putting the glass MOT vacuum tube in place. 16
5 Plot of the intensity distribution along the z-axis of a 780-nm laser beam incident upon a circular aperture with radius 75-μm and through a 0.1-m focal length lens. The relative intensity are depicted by colors ranging from the red-detuned traps with the highest intensity in red and the blue-detuned traps with the lowest intensity in violet. 17
6 Plot found using the original setup of scanning the pattern pixel by pixel. 18
7 Plot of the intensity distribution along the z-axis of a 780-nm laser beam incident upon a circular aperture with radius 75 μm and through a 0.075-m focal length lens. The relative intensity is depicted by colors ranging from the red-detuned traps with the highest intensity in the red and blue-detuned traps with the lowest intensity in violet. 19
8 Projection of pattern creating the primary blue-detuned-trap without the glass tube where a = 25 μm, f = 40 mm, L = 58.5 mm, and λ = 632.8 nm. 20
9 Projection of pattern creating the primary red-detuned-trap without the glass tube where a = 25 μm, f = 40 mm, L = 58.5 mm, and λ = 632.8 nm. 21
10 Projection of pattern creating the primary blue-detuned-trap through glass tube where a = 25 μm, f = 40 mm, L = 58.5 mm, and λ = 632.8 nm. 21
11 Projection of pattern creating the primary red-detuned-trap through glass tube where a = 25 μm, f = 40 mm, L = 58.5 mm, and λ = 632.8 nm. 22

12 Projection of pattern creating the primary red-detuned-trap through glass tube where a = 25 μm, f = 40 mm, L = 58.5 mm, and λ = 632.8 nm. 22
13 Projected diffraction pattern using 40 mm lens. 25
14 Projected diffraction pattern using 40 mm lens. 25
15 Projected diffraction pattern using 40 mm lens. 26
16 Projected diffraction pattern using 40 mm lens. 26
17 Projected diffraction pattern using 40 mm lens. 27
18 Projected diffraction pattern using 40 mm lens. 27
19 Projected diffraction pattern using 40 mm lens. 28
20 Projected diffraction pattern using 40 mm lens. 28
21 Projected diffraction pattern using 40 mm lens. 29
22 Projected diffraction pattern using 40 mm lens. 29
23 Projected diffraction pattern using 40 mm lens. 30
24 Projected diffraction pattern using 40 mm lens. 30
25 Projected diffraction pattern using 40 mm lens. 31
26 Projected diffraction pattern using 40 mm lens. 31
27 Projected diffraction pattern using 100 mm lens. 33
28 Projected diffraction pattern using 100 mm lens. 33
29 Projected diffraction pattern using 100 mm lens. 34
30 Projected diffraction pattern using 100 mm lens. 34
31 Projected diffraction pattern using 100 mm lens. 35
32 Projected diffraction pattern using 100 mm lens. 35
33 Projected diffraction pattern using 100 mm lens. 36
34 Projected diffraction pattern using 100 mm lens. 36
35 Projected diffraction pattern using 100 mm lens. 37
36 Projected diffraction pattern using 100 mm lens. 37
37 Projected diffraction pattern using 100 mm lens. 38
38 Projected diffraction pattern using 100 mm lens. 38

39 Projected diffraction pattern using 100 mm lens. 39
40 Projected diffraction pattern using 100 mm lens. 39
41 Projected diffraction pattern using 100 mm lens. 40
42 Projected diffraction pattern using 100 mm lens. 40
43 Projected diffraction pattern using 100 mm lens. 41
44 Projected diffraction pattern using 100 mm lens. 41
45 Projected diffraction pattern using 100 mm lens. 42
46 Projected diffraction pattern using 100 mm lens. 42
47 Projected diffraction pattern using 100 mm lens. 43
48 Projected diffraction pattern using 100 mm lens. 43
49 Projected diffraction pattern using 100 mm lens. 44

Acronym/Symbol	Meaning
a	Aperture Radius
BDT	Blue-Detuned Trap
f	Focal Length of Lens
HVDT	Hertz Vector Diffraction Theory
L	Axial Distance Between the Diffraction Aperture and the Lens
λ	Wavelength
MOT	Magneto Optical Trap
$\vec{r}_0$,(x_0, y_0, z_0)	Point in the Aperture Plane
$\vec{r}_1$,(x_1, y_1, z_1)	Point of Interest
$\vec{r}_L$,(x_L, y_L, z_L)	Point in the Lens Plane
RDT	Red-Detuned Trap
z	Distance from Lens Along the z-axis

Table 1: Acronyms and Symbols

1 Abstract

Theoretical calculations were performed for the projection of a diffraction pattern created by a pinhole through a single-lens system using vector diffraction theory and a combination of programs (MathCAD, Igor, etc.). The projected diffraction patterns were then experimentally created, recorded, and analyzed. This work is part of a larger collaboration with Dr. Kat Gillen, to trap and manipulate atoms in a Magneto Optical Trap (MOT) and to make further steps in the direction of Quantum Computing using trapped neutral atoms.

The final goal of this experiment is to determine whether or not the projected patterns created using the optical trapping system, as previously described, will be affected by the placement of a thin piece of cylindrical glass tube, such as that of the outer glass walls of a vacuum chamber housing a MOT. In order to do this, I created a data base of optical trap patterns by manipulating different parameters in the optical system without the placement of the cylindrical glass tube. I then found similar traps with the glass tube in place while using the same combination of experimental parameters. This allowed me to compare the two cases so as to determine any affects from the glass tube on the patterns.

2 Introduction

The optical dipole force is the theoretical foundation for the atom traps created in this experiment [1]. The optical dipole force is created by the interaction of the oscillating electric field of laser light with individual atoms. With this force, atoms can be trapped in localized high-intensity and low-intensity light fields. Whether the atom is draw to the high or low-intensity field is determined the laser's frequency and the atoms resonant dipole frequency. If the laser's frequency is greater than the atom's resonant dipole frequency, the dipole potential energy is a maximum for localized high-intensity fields thus creating a blue-detuned trap (BDT) [2]. If the laser's frequency is less than the atom's resonant dipole frequency, the opposite will occur where the dipole potential energy is a minimum for localized high-intensity fields creating a red-detuned trap (RDT) [2].

In order to take advantage of this force a method for creating localized light maxima or minima must be decided upon. There are multiple methods which have been used in the past to create optical traps. Utilizing a newer method, the experiment involves a process of diffracting light using a spatially limiting

aperture [2] [3]. The diffracted light then creates a series of localized high-intensity and low-intensity fields close enough to the aperture to use Hertz vector diffraction theory (HVDT) [4]. HVDT then allows calculations to be made of the theoretical position of the RDT and BDT traps [5]. This method proves to be advantageous due to the fact that the setup is quite simple compared to other methods which typically require tightly focused laser beams as well as the fact that switching between RDT and BDT traps is as simple as changing the laser's frequency [2].

One issue with this setup is that the traps are too close to the aperture to allow for a vacuum chamber of a magneto-optical trap (MOT) to be placed in the system without having the aperture incorporated into the chamber itself. Incorporating the aperture into the design of the chamber would create problems with swapping the aperture as this would require venting the vacuum chamber. Due to the fact that venting an ultra-high vacuum chamber and baking it out takes a significant amount of time, this is not a reasonable idea [2].

Another issue arises when trying to change the size, shape, position or any number of other properties of the traps. The only variable that can manipulate these properties is the size of the aperture being used [2]. In order to have more variation and control over these parameters, we need to introduce another experimentally controlled parameter.

Using a lens to image the pattern away from the aperture and into free space such as a MOT cloud inside of a vacuum chamber takes care of both issues. The traps are moved as far away from the chamber as necessary allowing room to work and keeping the vacuum chamber clean and at the necessary vacuum level for trapping atoms. Incorporating a projection lens into the optics also introduces two a handy variables into the system the position and the focal length of the lens allowing the manipulation of multiple properties of the traps.

3 Theory

3.1 RDT and BDT Traps

Light behaves as both a wave and a particle. Observation of particle or wave behavior is entirely dependent on how the experiment is being conducted. For this investigation, light is considered to be a wave with behaviors including polarization, interference, and diffraction. There are a few different methods

for creating the necessary diffraction pattern to create optical atom traps. In the end, the most reasonable and precise method for creating a suitable diffraction pattern is to use a single beam through a pinhole and using the emerging pattern on the other side. Diffraction of light through a circular aperture creates a series of localized maxima intensity fields, or red-detuned traps (RDT), and localized minima intensity fields, or blue-detuned traps (BDT), which allow for trapping cold atom with low energies [2]. The trap properties are also dependent on the frequency of the laser and the resonant frequency of the atoms being used. If the laser's frequency is less than the resonant frequency of the atoms, the atoms will be attracted to the high-intensity fields (RDT) [2]. If the laser's frequency is greater than the resonant frequency of the atoms however, the atoms will only be attracted to the low-intensity fields (BDT) [2].

3.2 Determining a Model

The first step is to determine a model for which the diffraction pattern is most accurate under the circumstances. The proximity of the point of interest, either the red detuned trap or blue detuned trap, to the diffracting aperture plays a significant role in determining what mathematical approximations, and hence which model should be used for this experiment. The traps of interest for this investigation exist less than 2-mm from the aperture [2]. Employment of Hertz vector diffraction theory (HVDT) was used to start, as its region of validity includes all space within the diffracting aperture and beyond. Thus, it is a natural starting point for conducting calculations for the regions of close proximity to the aperture. HVDT gives us the pattern of red detuned traps and blue detuned traps illustrated in figure 1.

The pattern of traps which appears in figure 1 was found just after the circular aperture. The z-axis, measured in microns, begins at the face of the aperture and measures away from it in the direction of the beams propagation. The y-axis is referred to more commonly as the r-axis in this paper and the normalized intensity, S_z/S_o, was found by dividing the relative intensities in the diffraction pattern by the plane wave intensity incident upon the circular aperture. The largest, most easily identifiable RDT and BDT are those which we will be concentrating on in this experiment. These are the first violet spot centered from the right (BDT) and the first red, full spot centered from the right in figure 1. They are known as the primary red-detuned trap and primary blue-detuned trap. Both the primary RDT and BDT sites are far enough away from the aperture to allow the Fresnel approximation to be employed since it allows for simpler calculations without compensating for accuracy [2]. Additionally, the Fresnel

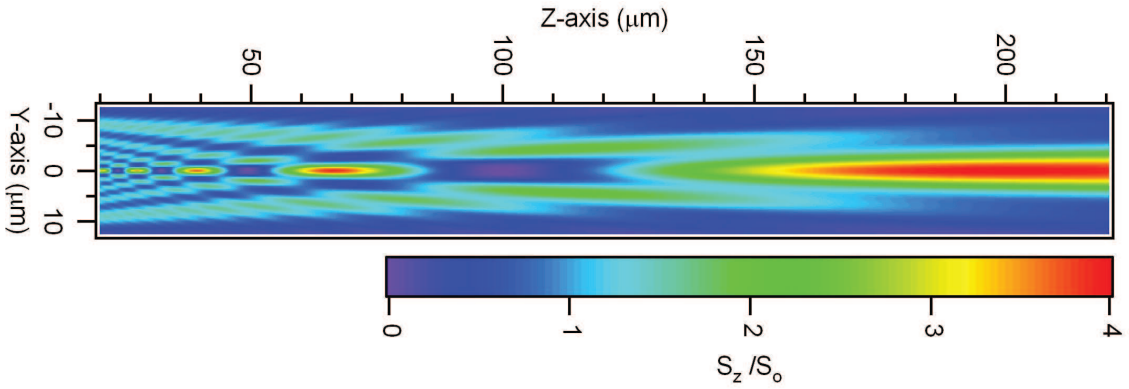

Figure 1: Plot of the intensity distribution along the z-axis of a 780-nm laser beam incident upon a circular aperture with radius 25-μm. The relative intensities are normalized and are depicted by colors ranging from the red-detuned traps with the highest intensity and the blue-detuned traps with the lowest intensity [5].

approximations will suffice since the distance to the lens from the pinhole is large and are within the Fresnel approximation. Mathematically we find that the locations of the RDT and BDT traps of interest lie within the Fresnel approximation [2] or,

$$z_1^3 \gg \frac{\pi}{4\lambda}\left[(x_1 - x_0)^2 + (y_1 - y_0)^2\right]^2, \tag{1}$$

where λ is the wavelength of the beam light, x_1, y_1, and z_1 are the point of interest, and x_0 and y_0 are the location of an integration point in the aperture plane. Thus, we can use a simpler and computationally faster Fresnel diffraction model for the projected diffraction pattern.

3.3 Propagation Through Lens

The main diffraction patterns, created by passing light waves through a pinhole, only exist millimeters away from the pinhole itself. Unfortunately, this will not suffice as we need the pattern to be projected into the glass vacuum chamber tube housing the MOT. The logical answer for this is to use a lens to create a real image of the pattern on the other side of the lens. With this lens in place, we can easily manipulate the size, and location of any traps created.

The Fresnel approximation in cylindrical coordinates, for the point of interest in the diffraction pattern after the lens can be expressed as

$$E(r,z) = -\frac{k^2 e^{ik(z+L)}}{LZ} \exp\left(\frac{ikr^2}{2z}\right) \int_0^R \left[\int_0^a E_{z_0} J_0\left(\frac{kr_0 r_L}{L}\right) \exp\left(\frac{ikr_0^2}{2L}\right) r_0 dr_0\right] \times J_0\left(\frac{kr_L r}{z}\right) \exp\left[i\frac{k}{2}\left(\frac{1}{L}+\frac{1}{z}-\frac{1}{f}\right) r_L^2\right] r_L dr_L, \quad (2)$$

where k is the wavenumber, R is the radius of the lens, E_{z0} is the distribution of the incident electric field with the open aperture area, J_0 is a Bessel function of the first kind of order zero, f is the focal length of the lens and r_L is the radial location of a point in the plane of the lens. However, since the size of the lens is significantly larger than the light distribution in the lens plane the limit of the dr_L integral effectively goes to infinity yielding another Bessel function. Equation 2 can be simplified down to

$$E(r,z) = \frac{dke^{ik(z+L)}}{iLz} \exp\left[i\frac{k}{2z}\left(1-\frac{d}{z}\right) r^2\right] \int_0^a E_{z_0} J_0\left(\frac{kr_0 rd}{Lz}\right) \exp\left[i\frac{k}{2L}\left(1-\frac{d}{L}\right) r_0^2\right] r_0 dr_0, \quad (3)$$

where d represents a relationship among the usual geometrical parameters L, z, and f by

$$d = \left[\frac{1}{L}+\frac{1}{z}-\frac{1}{f}\right]^{-1}. \quad (4)$$

Equation 3 yields the electric field at a point of interest in the MOT cloud of atoms.

From equation 3 the exact locations of on-axis maxima and minima can be predicted to occur when

$$z = f\frac{1-nL\frac{\lambda}{a^2}}{1-n(L-f)\frac{\lambda}{a^2}}, \quad (5)$$

where n is an integer and λ is the wavelength of the incident laser light. If n is an odd number the corresponding optical dipole potential energy will have a maximum for RDT traps, and if n is even the potential energy will have a minimum for BDT traps. In figure 5, the primary RDT trap corresponds with n = 3 and the primary BDT trap corresponds with n = 2. Equation 5 can be written in a more convenient form to resemble the thin lens equation as

$$\frac{1}{z} + \frac{1}{L-\frac{a^2}{n\lambda}} = \frac{1}{f}. \quad (6)$$

3.4 Projection into MOT

One of the major goals of this experiment is to image the diffraction pattern, using a thin lens, through the glass wall of the vacuum chamber and into the MOT cloud of atoms where the primary RDT (or primary BDT) potential energy well will trap a single atom. The lens will not be an issue as far as distortions to the traps, however, once they are formed on the other side of the lens, the traps must still be projected through the thin cylindrical glass wall of the vacuum chamber. At this instance, the traps could experience refraction, interference of multiple internal reflections within the glass and/or any number of other possible distortions.

It is important to investigate any distortions to the traps' shapes and sizes prior to setting up a finalized MOT system, since the process of assembling and disassembling a MOT is a very tedious task in itself. By viewing images of the patterns inside the glass chamber while the system is disassembled, we are able to determine potential problems before they become serious ones.

4 Experimental Setups

The theoretical setup for projections of the diffraction patterns created near the metallic aperture, imaged through a lens and finally projected into a cloud in a MOT is seen in figure 2 where the important parameters are: radius a of the aperture, axial distance L between the diffracting aperture and the lens, and axial distance z between the lens and the point of interest. The outcome of this setup and implementation of the Fresnel approximation is seen in figure 5.

4.1 Imaging Setups

In order to find better images of the BDT and RDT traps, a CCD camera was connected to a computer running National Instruments Measurement and Automation Explorer. This program allows the capturing of higher resolution images than the pixel by pixel scanning process used previously. Once the trap images were scanned into the database, Igor was used to convert the r-axis from pixel number, as collected by the National Instruments program, into S.I. units after finding the micron per pixel conversion for the CCD camera. The Igor program was also used to magnify the image of the trap and finally label each image with the corresponding a, λ, L, and z variables. This allowed for easier comparison of these

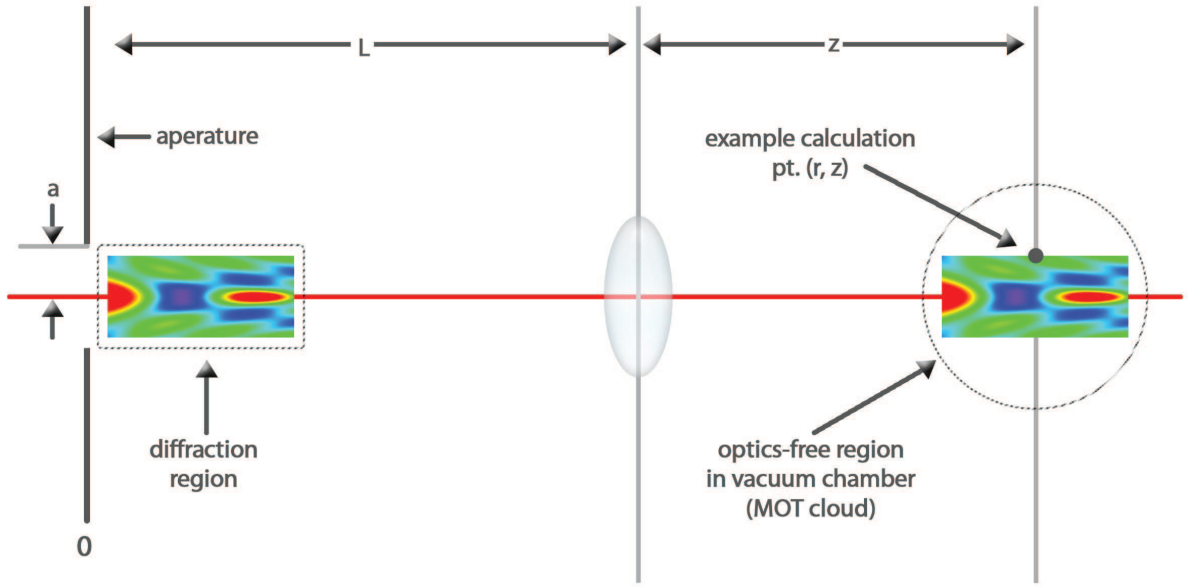

Figure 2: Theoretical setup for near-field diffraction patterns to an vacuum chamber holding a MOT cloud of cold atoms.

images once the database was completed.

The new setup for determining the size and location of RDT and BDT traps can be seen in figure 3 where the diffraction patterns are projected directly onto the CCD camera, rather than the scanning setup which proved to be inefficient. Moving the camera along the z-axis allows pictures to be taken at different intervals.

4.1.1 Equipment List

- 5mW HeNe Laser (JDS Uniphase 1507P-0)
- Variable Polarizer
- Optical Hardware
- Optical Rail
- 40mm, 50mm, 75mm, and 100mm Focal Length Lenses
- 25μm, 50μm, 75μm, and 100μm Pinhole Apertures

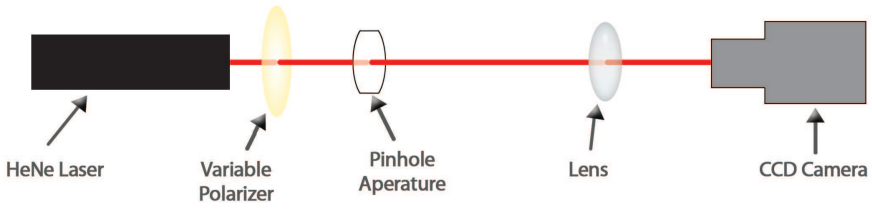

Figure 3: Experimental setup for finding RDT and BDT traps.

- CCD Camera (COHU Solid State Camera)

4.2 Glass Vacuum Chamber Setup and Implementation of the Cage System

When starting this experiment, the entire system setup used posts and post holders on a rail system. This worked great for the time being but when looking into the future of the project, this system would prove difficult to use. To achieve the best results when moving the system from the original setup to the location of the experiment where the MOT cloud will be created a cage system had to be incorporated. This system would allow locking the lens and aperture into a single system rather than allowing them to shift during transportation. The cage system is another way to make this experiment as simple as possible for changing out lenses and apertures.

Once a collection of images without the glass tube in place was finished, the glass tube and cage system were placed into the system as seen in figure 4 where the tube's surface is placed perpendicular to the incident beam and then is reflected by a mirror placed inside the tube at 45 degrees to the CCD camera where an image can be captured by the National Instruments program.

4.2.1 Equipment List

- 5mW HeNe Laser (JDS Uniphase 1507P-0)
- Variable Polarizer
- Optical Hardware

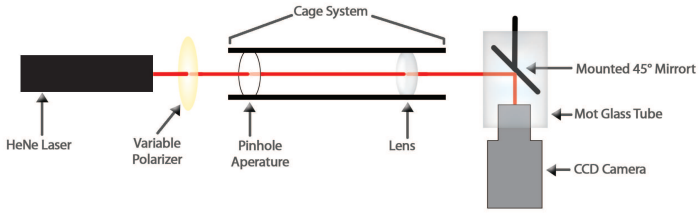

Figure 4: Experimental setup using a cage system and putting the glass MOT vacuum tube in place.

- Optical Rail
- Cage System and Optical Mounts
- 40mm, 50mm, 75mm, and 100mm Focal Length Lenses
- 25μm, 50μm, 75μm, and 100μm Pinhole Apertures
- CCD Camera (COHU Solid State Camera)
- Mirror Mounted at 45 degrees
- Glass Vacuum Chamber Tube with Opening on One Side

5 Results

5.1 Calculation and Computational Results

When first starting the process of capturing projected images of traps, MathCAD was use running on a Windows OS. With this program, the theoretical relationships between the variables were used to calculate the positions of large traps, which are easier to find, and small traps, which are ideal for trapping single atoms. These predicted positions were graphed using Igor along the z-axis to create images as in figure 5. Once these positions along the z-axis were determined, an image scan was taken of the region along r-axis using a pixel by pixel intensity scanning program. When the scan was completed, the Igor program was employed to combined the data into an image as seen in figure 6 and convert the r-axis from pixel number to S.I. units. This process proved to be very time consuming as each scan took one to two days to complete and the image quality was quite poor.

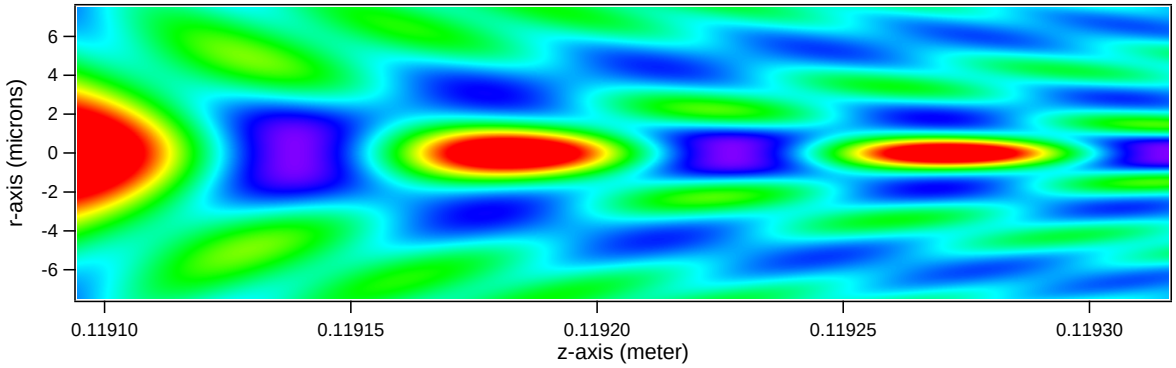

Figure 5: Plot of the intensity distribution along the z-axis of a 780-nm laser beam incident upon a circular aperture with radius 75-μm and through a 0.1-m focal length lens. The relative intensity are depicted by colors ranging from the red-detuned traps with the highest intensity in red and the blue-detuned traps with the lowest intensity in violet.

The result of using the MathCAD program designed by Glen Gillen was the creation of a database of projected diffraction patterns. The MathCAD program allowed for the manipulation of the L, a, λ, and f parameters so as to create variation in the pattern sizes and positions. These traps, graphed using Igor, ranged from dimensions of about 10 μm by 100 μm as in figure 7 to about 2 μm by 30 μm as in figure 5.

5.2 Experimental Results

The original setup using a scanning system to capture images of the RDT and BDT traps and worked great for small patterns (¡ 10s of μm) and allowed for sub-micron steps. Unfortunately, this setup was extremely slow in terms of data collection. The new setup as seen in figure 3 allowed for much faster data collection but it had its draw backs as well. Since the pixel size was about 12 μm, the patterns had to be much larger in order to view them clearly.

Figure BDT	Figure RDT	a (μm)	f (mm)	L (mm)	λ (nm)	z Primary BDT (mm)	z Primary RDT (mm)
20	15	25	40	58.5	632.8	≈ 142.1	≈ 146.1
33	28	75	100	170	632.8	≈ 258.20	≈ 277.80

Table 2: Primary RDT and Primary BDT Trap Images

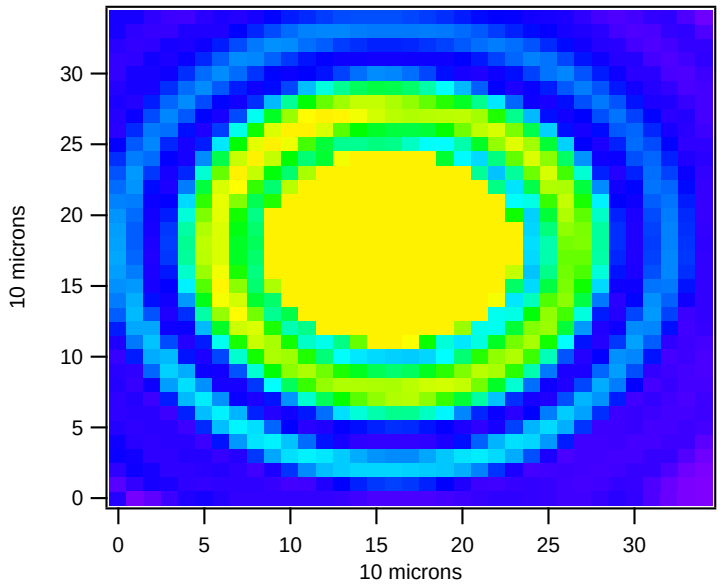

Figure 6: Plot found using the original setup of scanning the pattern pixel by pixel.

5.3 Projections to Determine Effects of Glass Vacuum Chamber Tube

Below in figure 8, we can see the projection of the primary blue-detuned-trap without being projected through the glass tube.

Figure 9 shows the primary red-detuned-trap found without the glass tube. Key notes about this and other figures in this section are the intensity and the shape of the traps.

Figure 10 shows the primary blue-detuned-trap found when projecting the pattern through the glass tube. This is what we will be looking for when the MOT is finished being setup.

Finally, in figure 11 we see the primary red-detuned-trap after the pattern has been projected through the glass vacuum chamber of the MOT. Note again the intensity and the shape of the trap. This too is the final outcome of the projections.

Using careful analysis, it was determined that as long as the beam is steered exactly perpendicular onto the tube's surface, the diffraction pattern should remain unaltered allowing the use of the traps inside the MOT atom cloud.

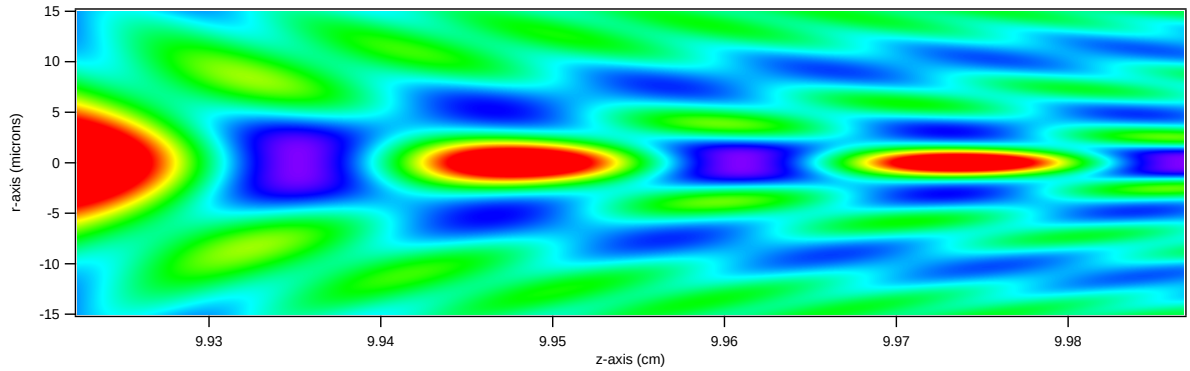

Figure 7: Plot of the intensity distribution along the z-axis of a 780-nm laser beam incident upon a circular aperture with radius 75 μm and through a 0.075-m focal length lens. The relative intensity is depicted by colors ranging from the red-detuned traps with the highest intensity in the red and blue-detuned traps with the lowest intensity in violet.

6 Discussion

When first attempting to find this projection of the diffraction pattern through the glass tube of the MOT, the image came out as in figure 12, which gives the impression that this traps will be distorted. However, after looking closely at the setup it was found that the beam had not been incident on the surface of the tube exactly perpendicular. Figure 12 is an example of what happens in such a case. Fixing this problem requires careful adjustment of the position of the chamber while having the camera on. This allows the visual confirmation that the glass chamber surface is perpendicular to the incident beam when the oval becomes a circle as found in figure 11 for RDT traps or in figure 10 for BDT traps.

7 Conclusions

In this experiment, we were able to determine two methods for locating RDT and BDT traps along the axis of beam propagation. One being the scanning setup and the other being the CCD camera setup, each with there respective advantages and disadvantages. Finally, by imaging the diffraction pattern through the glass vacuum tube, we found that it is necessary to project the beam exactly perpendicular to its cylindrical surface. There were no significant changes in the size or shape of the traps as long as this specification was met properly, as was seen when comparing multiple images of the patterns with the glass tube in place to those without. This corresponds with what was to be expected by the basics of

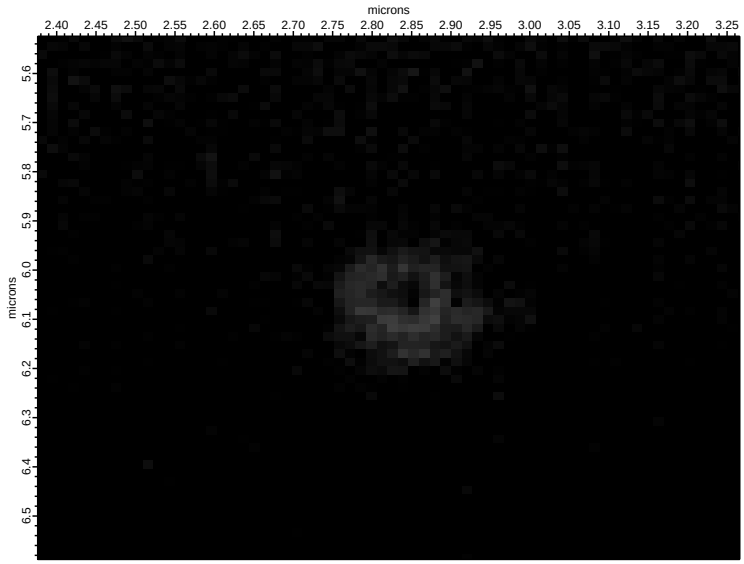

Figure 8: Projection of pattern creating the primary blue-detuned-trap without the glass tube where a = 25 μm, f = 40 mm, L = 58.5 mm, and λ = 632.8 nm.

geometrical optics as found in Pedrotti, Pedrotti, and Pedrotti's *Introduction to Optics*.

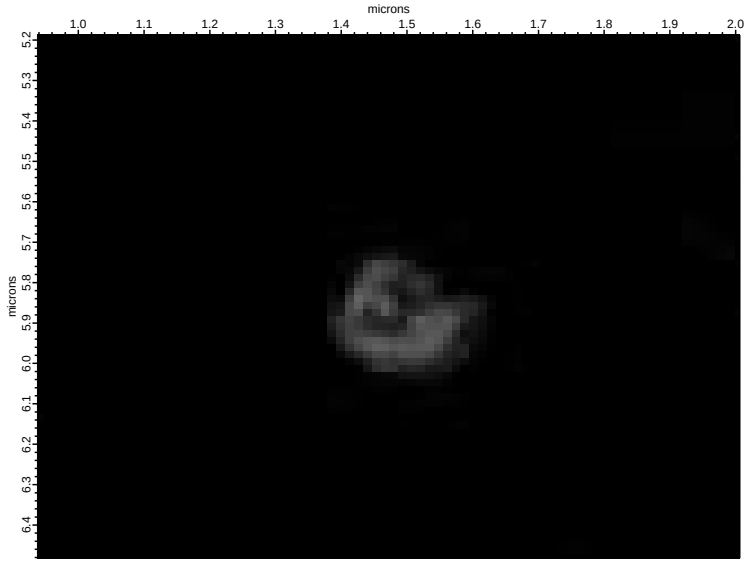

Figure 9: Projection of pattern creating the primary red-detuned-trap without the glass tube where a = 25 μm, f = 40 mm, L = 58.5 mm, and λ = 632.8 nm.

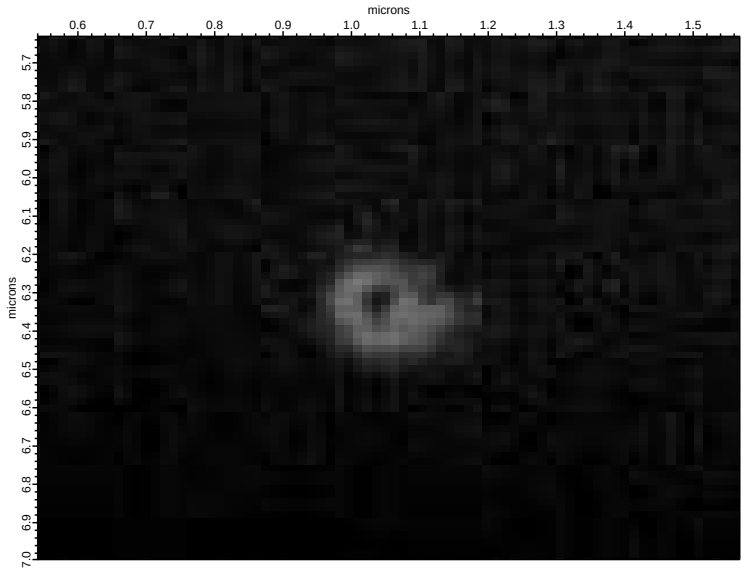

Figure 10: Projection of pattern creating the primary blue-detuned-trap through glass tube where a = 25 μm, f = 40 mm, L = 58.5 mm, and λ = 632.8 nm.

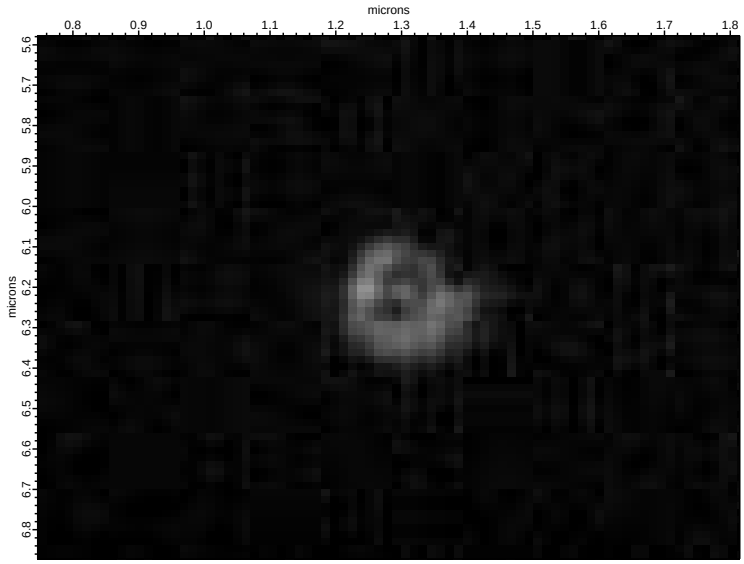

Figure 11: Projection of pattern creating the primary red-detuned-trap through glass tube where a = 25 μm, f = 40 mm, L = 58.5 mm, and λ = 632.8 nm.

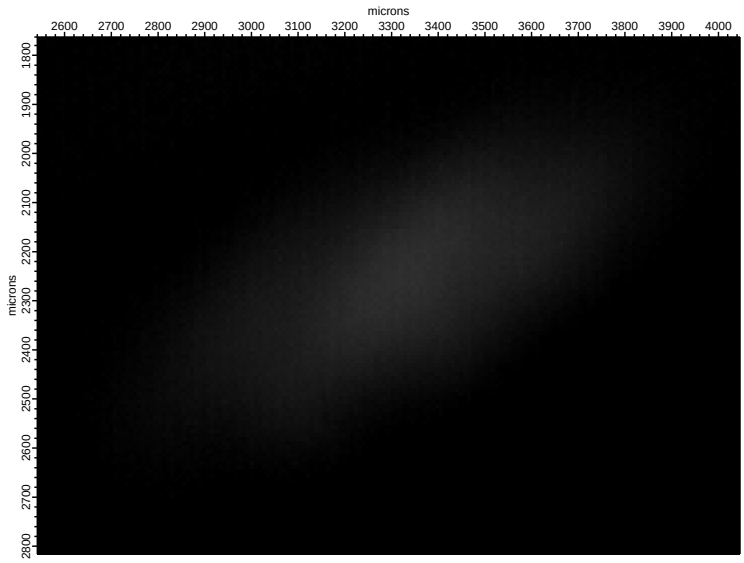

Figure 12: Projection of pattern creating the primary red-detuned-trap through glass tube where a = 25 μm, f = 40 mm, L = 58.5 mm, and λ = 632.8 nm.

References

[1] J. E. Bjorkholm, R. R. Freeman, A. Ashkin, and D. B. Pearson, "Observation of focusing of neutral atoms by the dipole forces of resonance-radiation pressure," Phys. Rev. Phys. Rev. Lett. **41**, 1361 (1978).

[2] Katharina Gillen-Christandl and Glen D. Gillen, "Projection of diffraction patterns for use in trapping cold neutral atoms," Phys. Rev. A **82**, 063420 (2010).

[3] L. Chen and J. Yin, "Improved far-field optical trap for cold atoms (molecules) with phase-modulated circular aperture diffraction," Phys. Rev. A **80**, 065401 (2009).

[4] V. V. Klimov and V. S. Letokhov, "New atom trap configurations in the near field of laser radiation," Opt. Comm **121** 130-136 (1995).

[5] G. D. Gillen, S. Guha and K. Christandl, "Optical dipole traps for cold atoms using diffracted laser light," Phys. Rev. A **73**, 013409 (2006).

[6] F. L. Pedrotti, L. S. Pedrotti, and L. M. Pedrotti, *Introduction to Optics*, Third Edition, (Person Prentice Hall, Upper Saddler River, NJ, 2007).

A 40 mm Lens Images

Using the setup as seen in figure 3 with a 40mm focal length lens, a 25μm radius aperture, a distance, L, of 58.5mm between them and a 632.8nm wavelength laser, figures 13 through 26 were found by moving a CCD camera along the z-axis of the imaged pattern. The primary BDT trap appears in figure 20 and the primary RDT trap appears in figure 15.

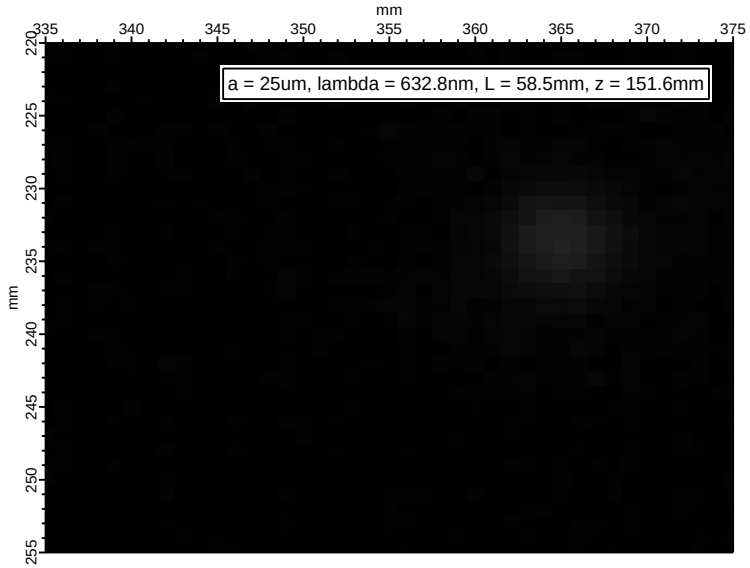

Figure 13: Projected diffraction pattern using 40 mm lens.

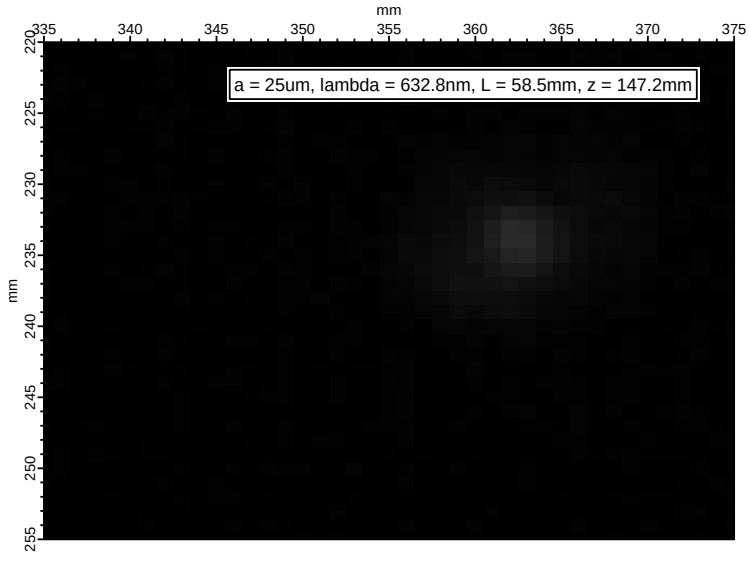

Figure 14: Projected diffraction pattern using 40 mm lens.

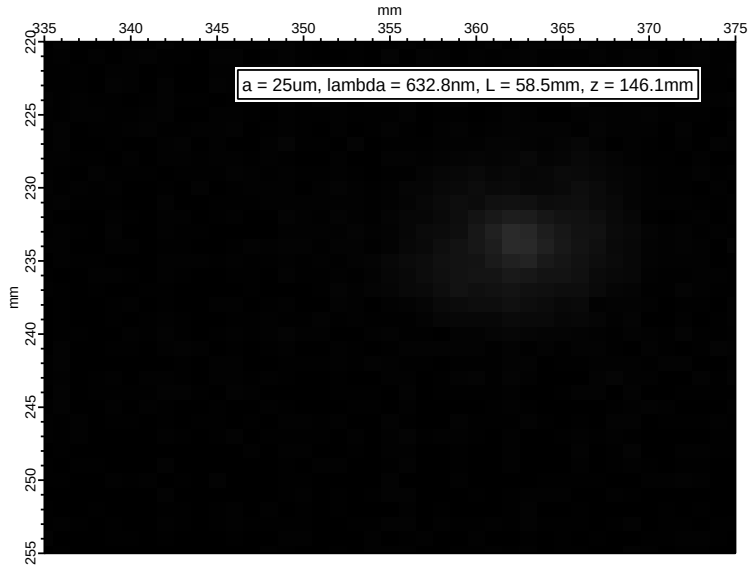

Figure 15: Projected diffraction pattern using 40 mm lens.

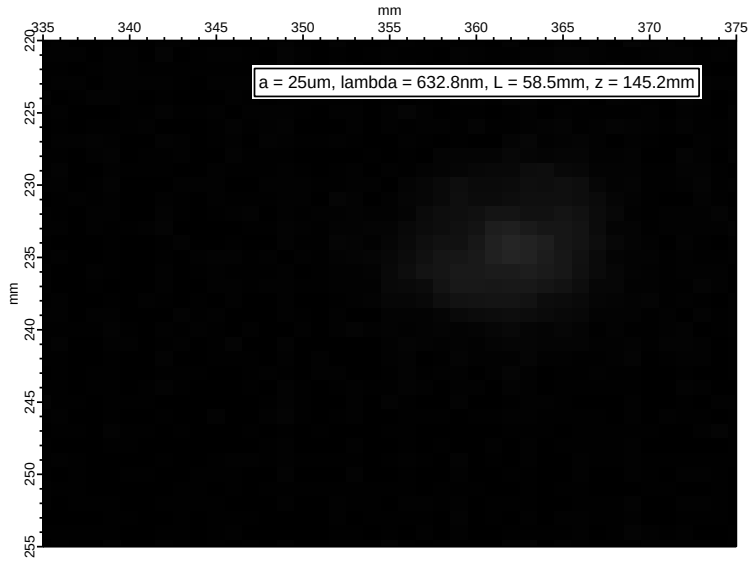

Figure 16: Projected diffraction pattern using 40 mm lens.

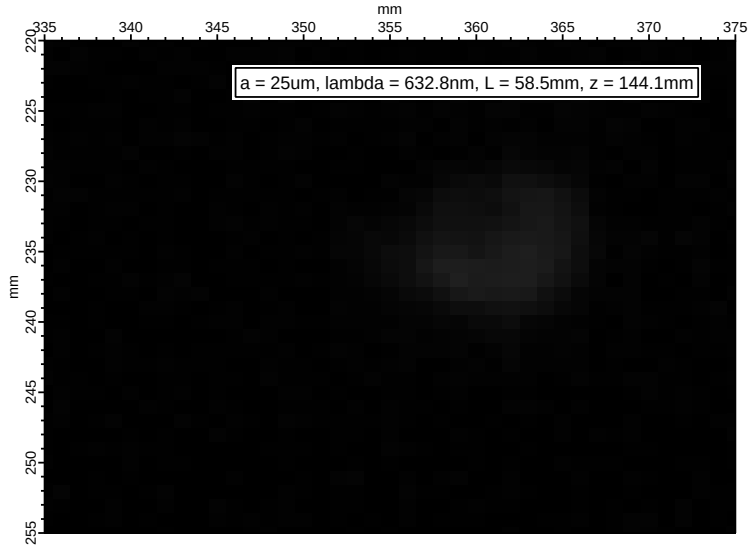

Figure 17: Projected diffraction pattern using 40 mm lens.

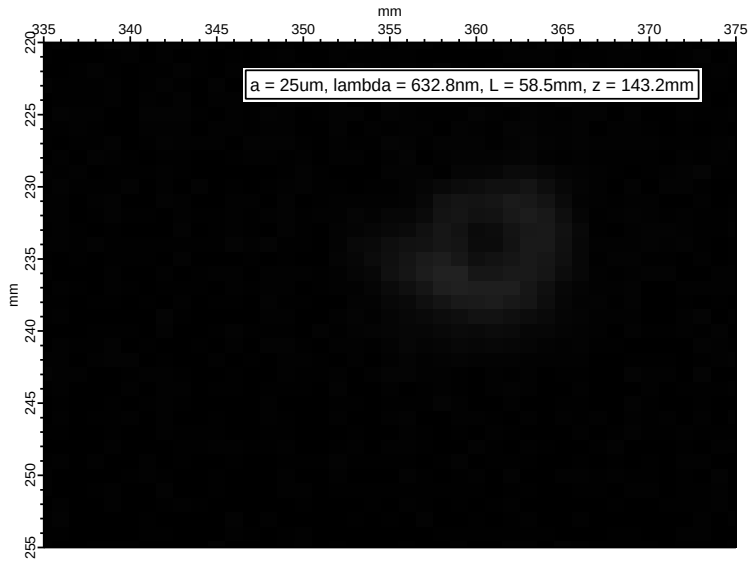

Figure 18: Projected diffraction pattern using 40 mm lens.

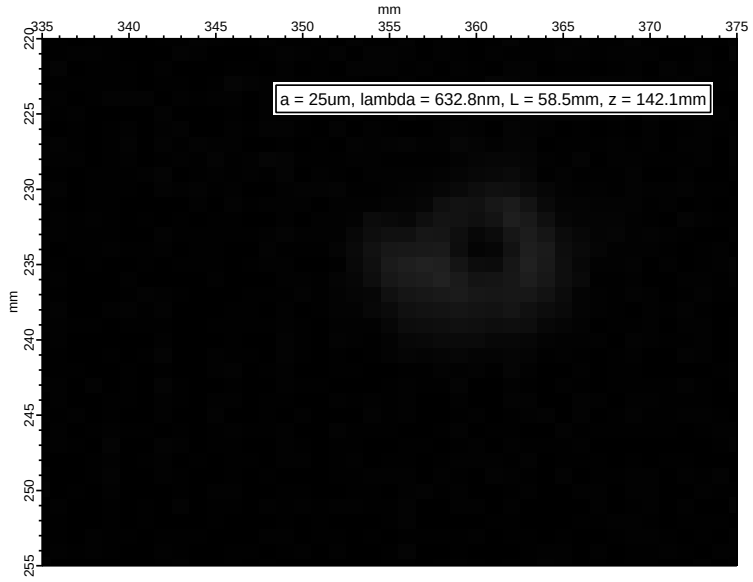

Figure 19: Projected diffraction pattern using 40 mm lens.

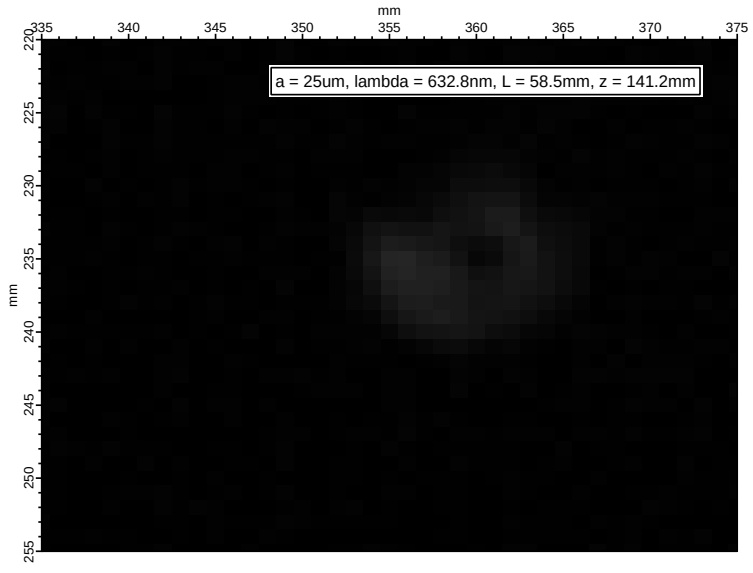

Figure 20: Projected diffraction pattern using 40 mm lens.

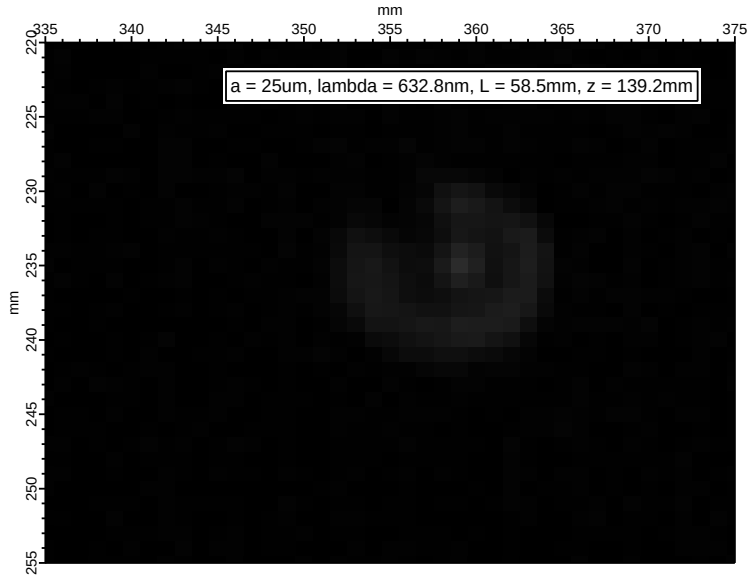

Figure 21: Projected diffraction pattern using 40 mm lens.

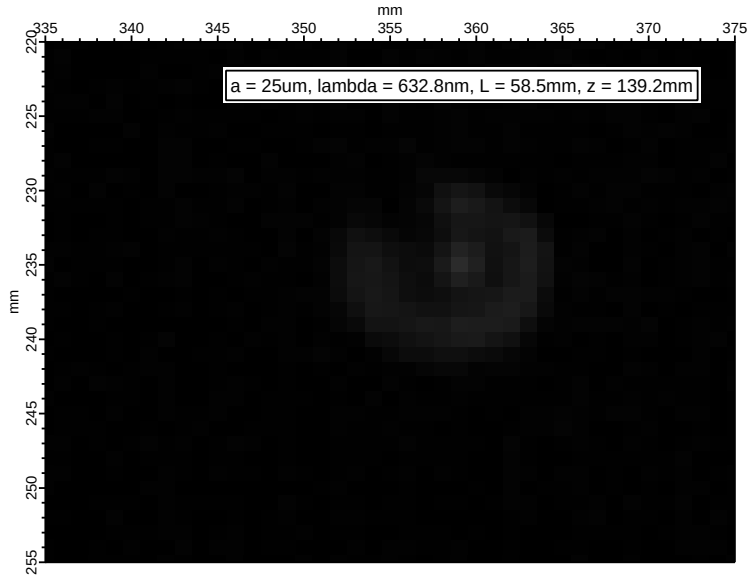

Figure 22: Projected diffraction pattern using 40 mm lens.

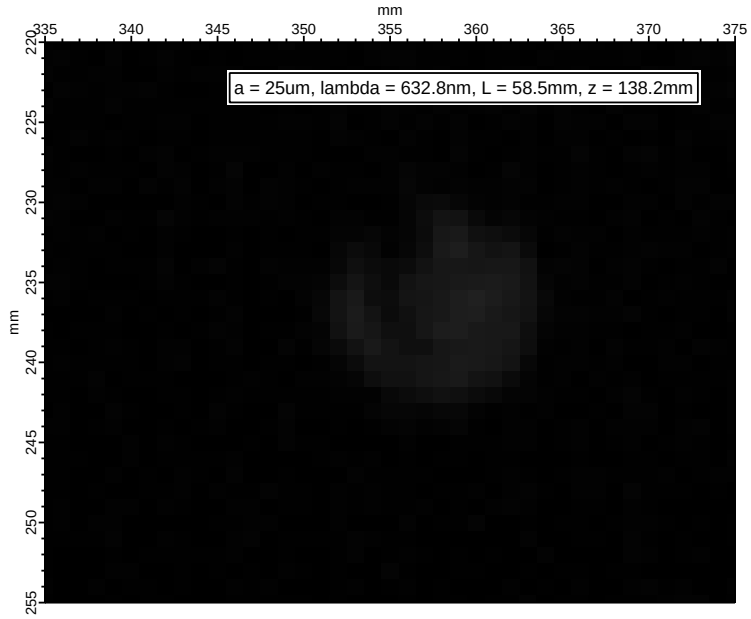

Figure 23: Projected diffraction pattern using 40 mm lens.

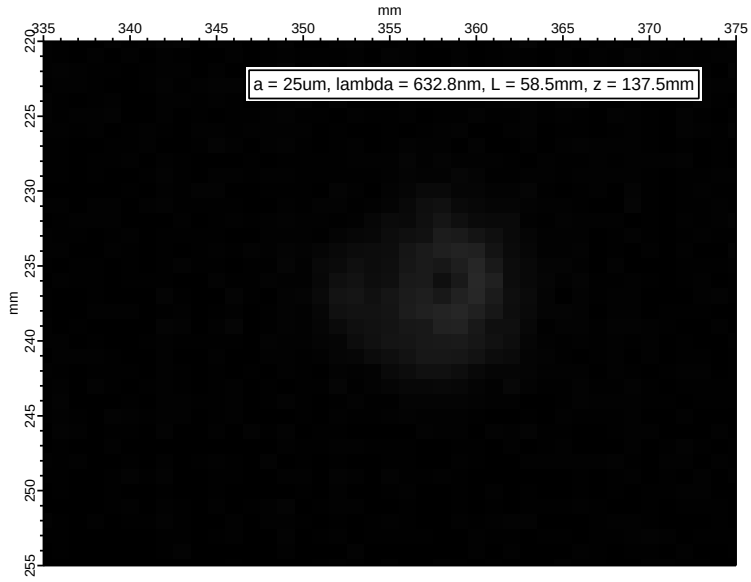

Figure 24: Projected diffraction pattern using 40 mm lens.

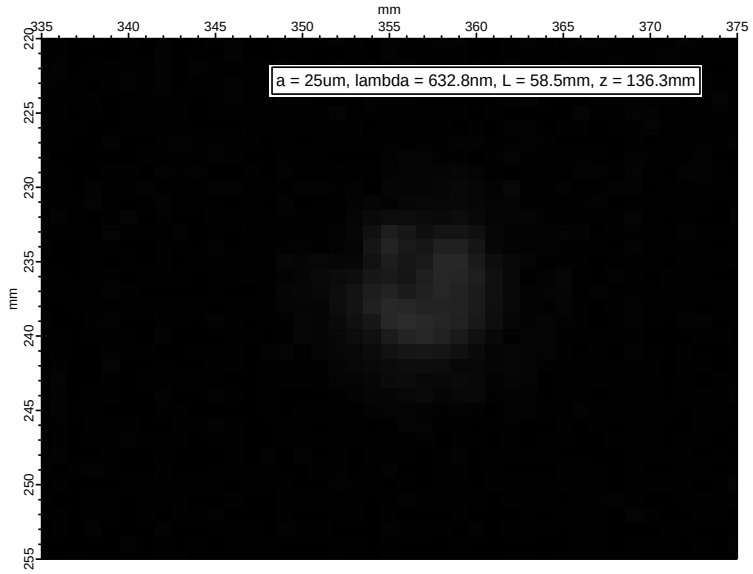

Figure 25: Projected diffraction pattern using 40 mm lens.

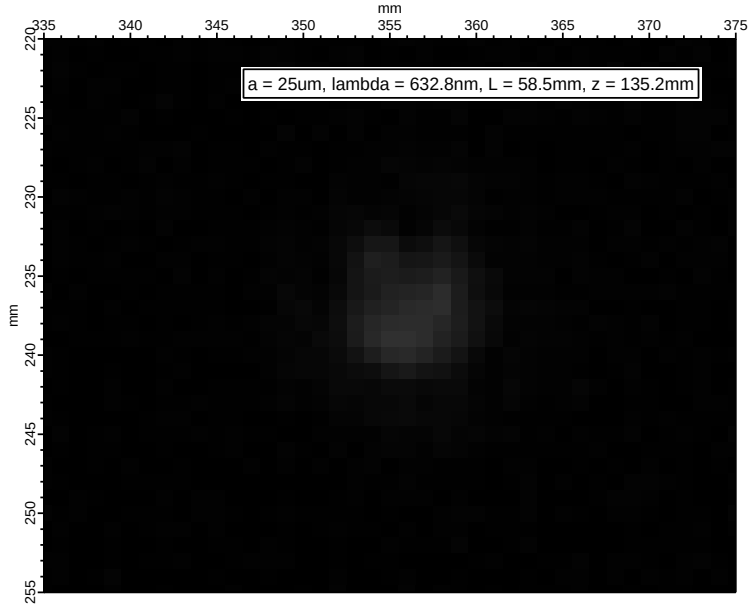

Figure 26: Projected diffraction pattern using 40 mm lens.

B 100 mm Lens Images

With the setup found in figure 3, where f is a 100mm focal length lens, a is a 75μm radius aperture, L is a distance of 170mm and λ is 632.8nm, figures 27 through 49 were found by moving a CCD camera along the z-axis of the imaged pattern. The primary BDT trap appears in figure 33 and the primary RDT trap appears in figure 28.

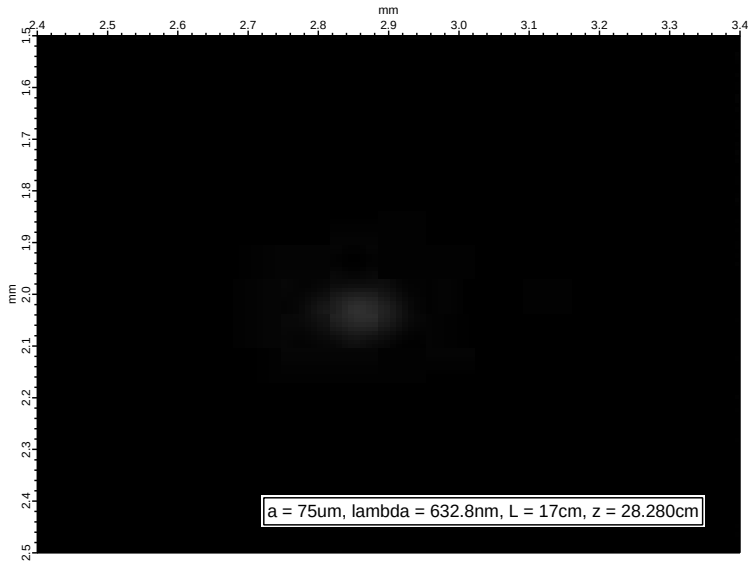

Figure 27: Projected diffraction pattern using 100 mm lens.

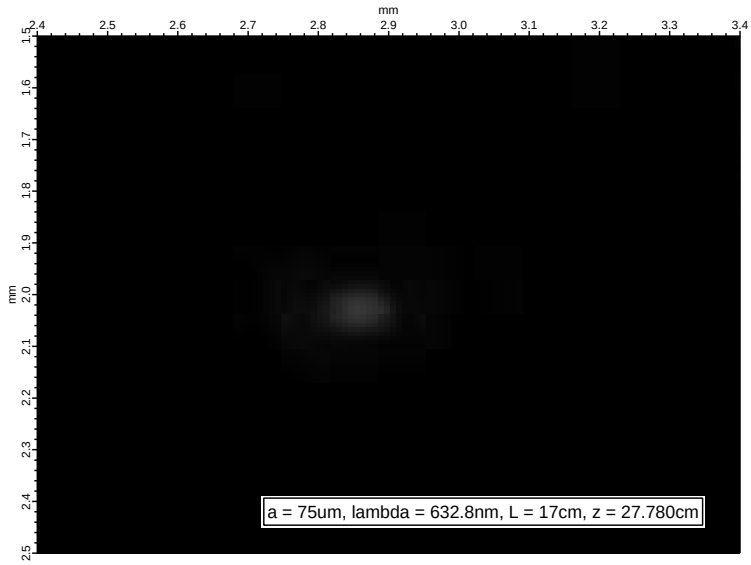

Figure 28: Projected diffraction pattern using 100 mm lens.

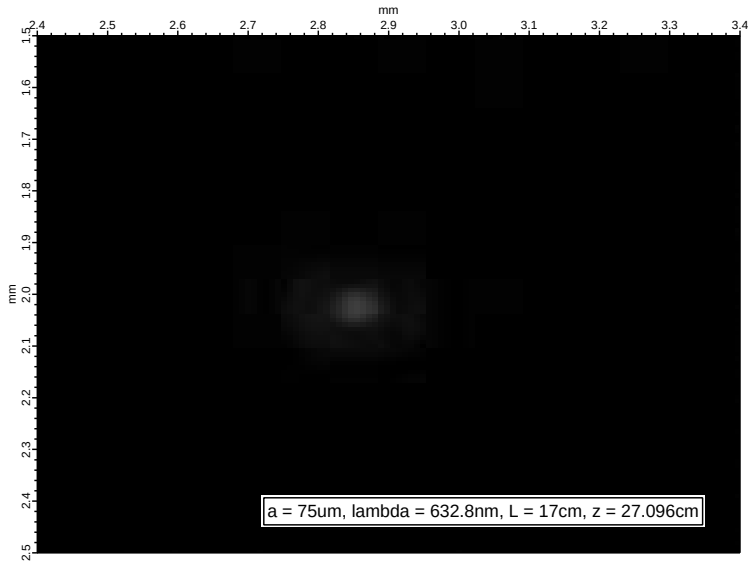

Figure 29: Projected diffraction pattern using 100 mm lens.

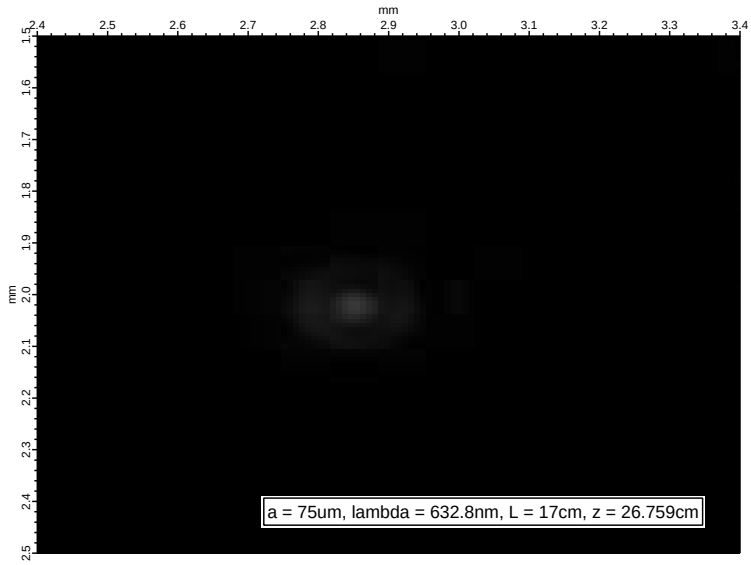

Figure 30: Projected diffraction pattern using 100 mm lens.

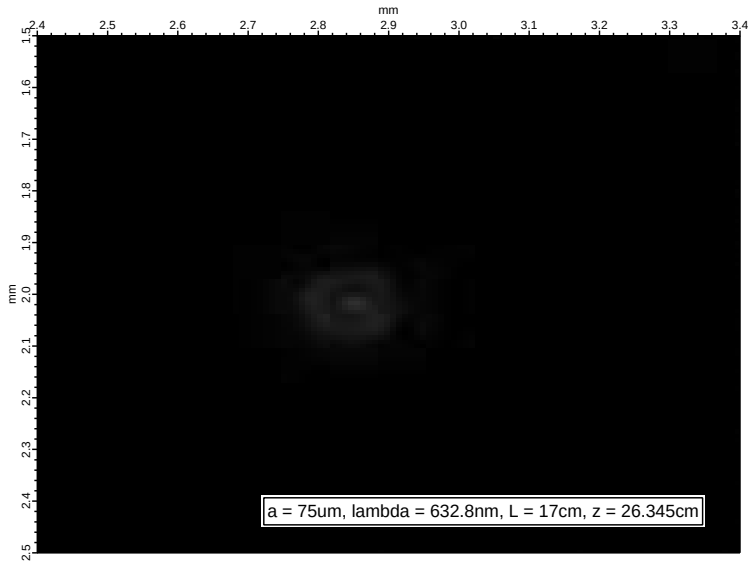

Figure 31: Projected diffraction pattern using 100 mm lens.

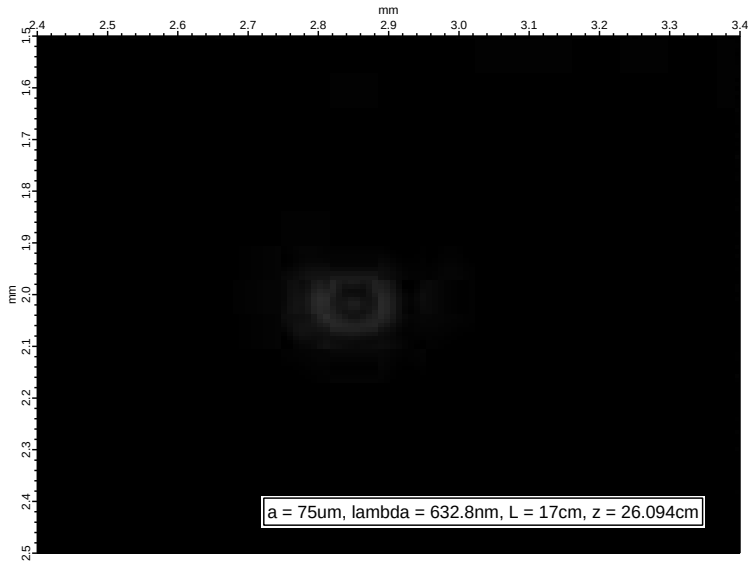

Figure 32: Projected diffraction pattern using 100 mm lens.

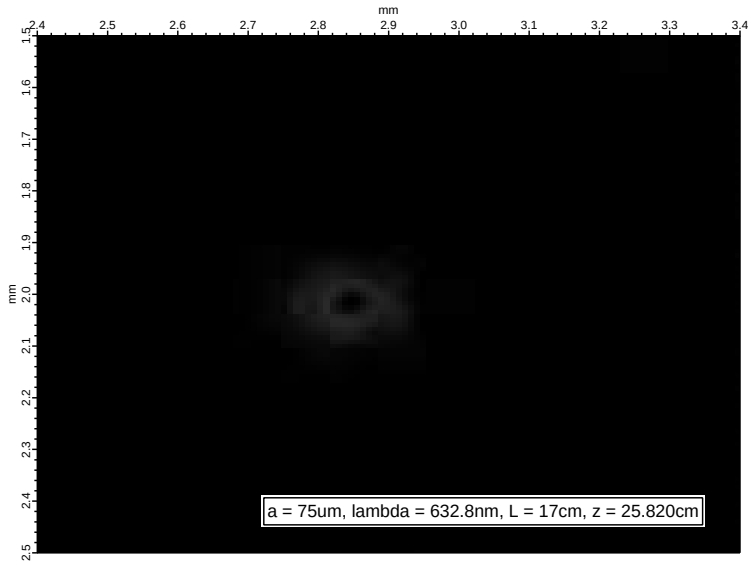

Figure 33: Projected diffraction pattern using 100 mm lens.

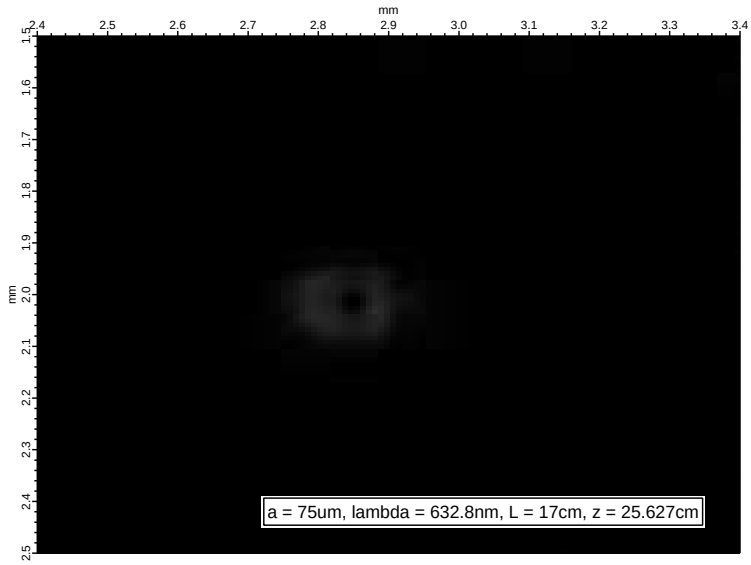

Figure 34: Projected diffraction pattern using 100 mm lens.

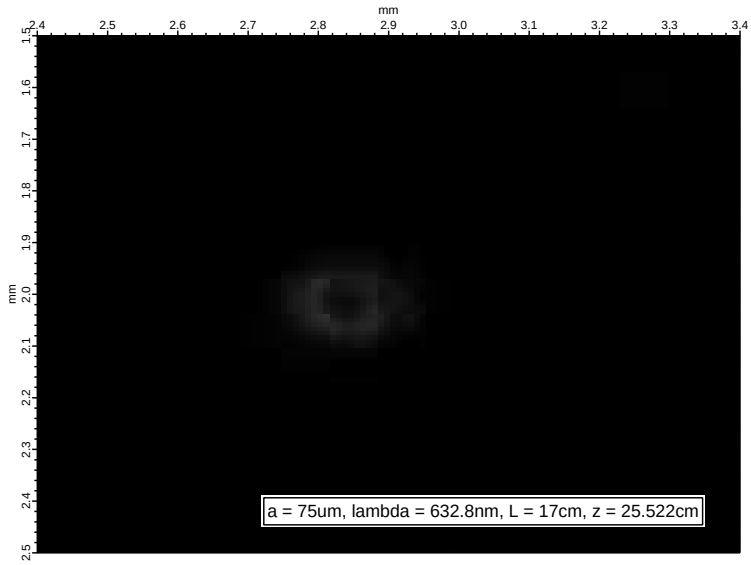

Figure 35: Projected diffraction pattern using 100 mm lens.

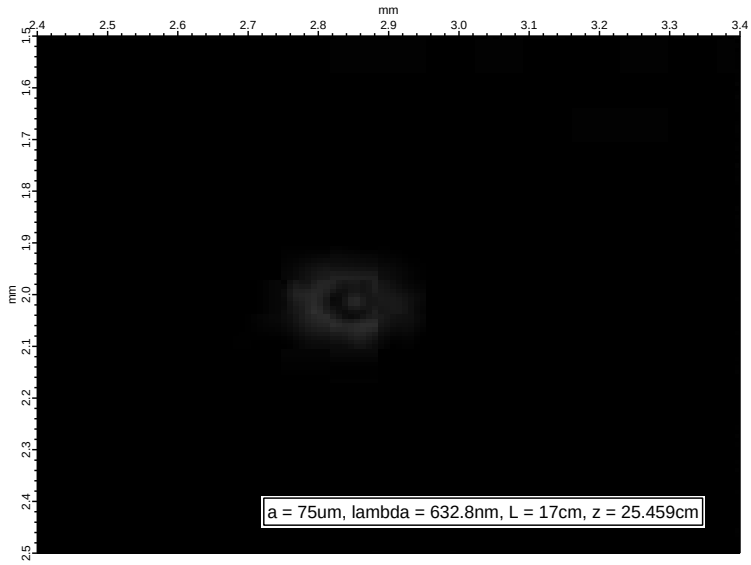

Figure 36: Projected diffraction pattern using 100 mm lens.

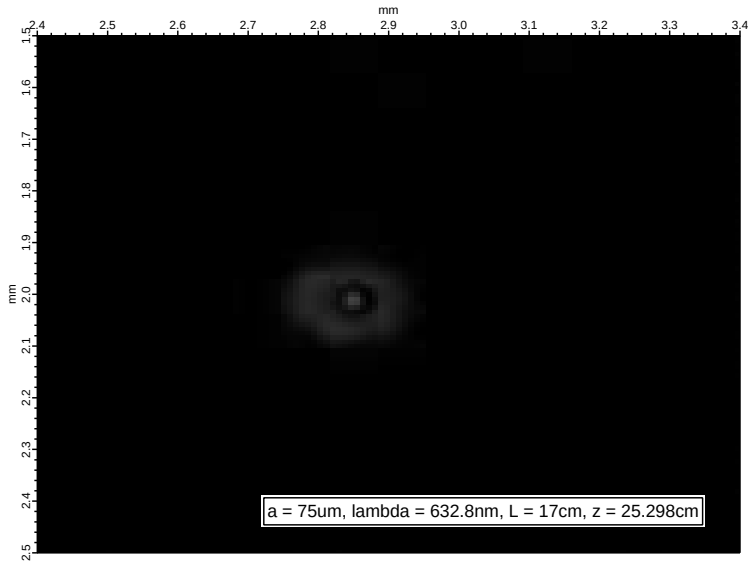

Figure 37: Projected diffraction pattern using 100 mm lens.

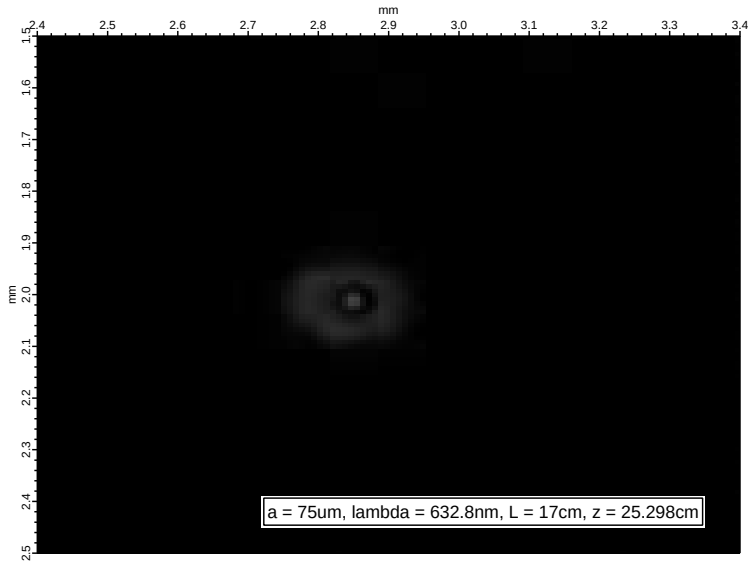

Figure 38: Projected diffraction pattern using 100 mm lens.

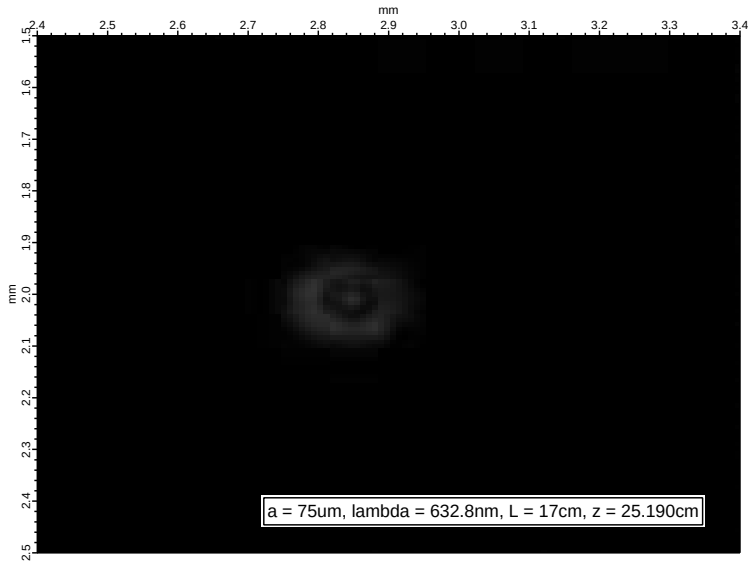

Figure 39: Projected diffraction pattern using 100 mm lens.

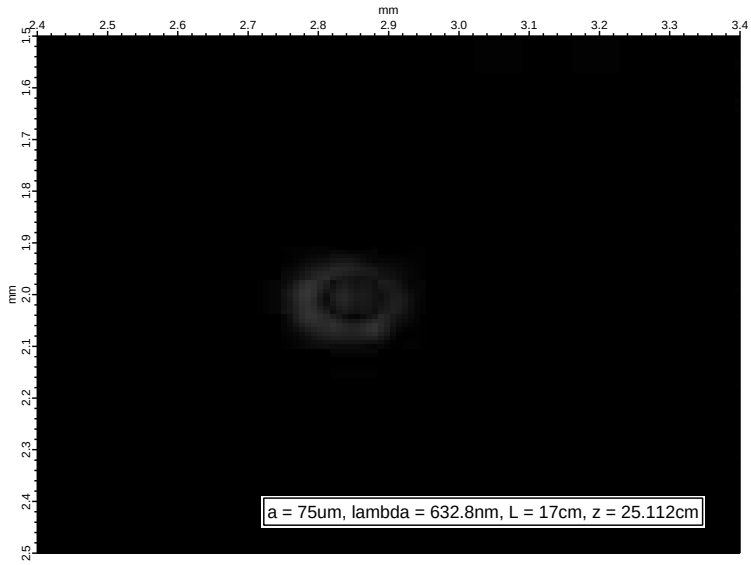

Figure 40: Projected diffraction pattern using 100 mm lens.

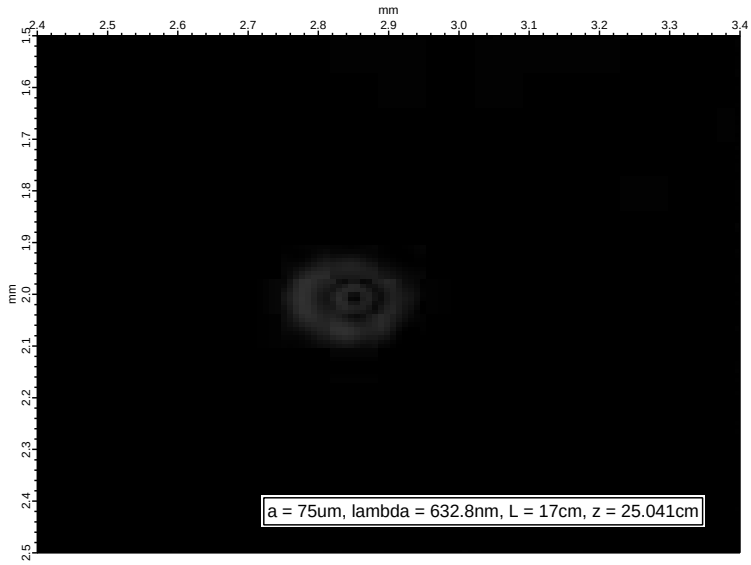

Figure 41: Projected diffraction pattern using 100 mm lens.

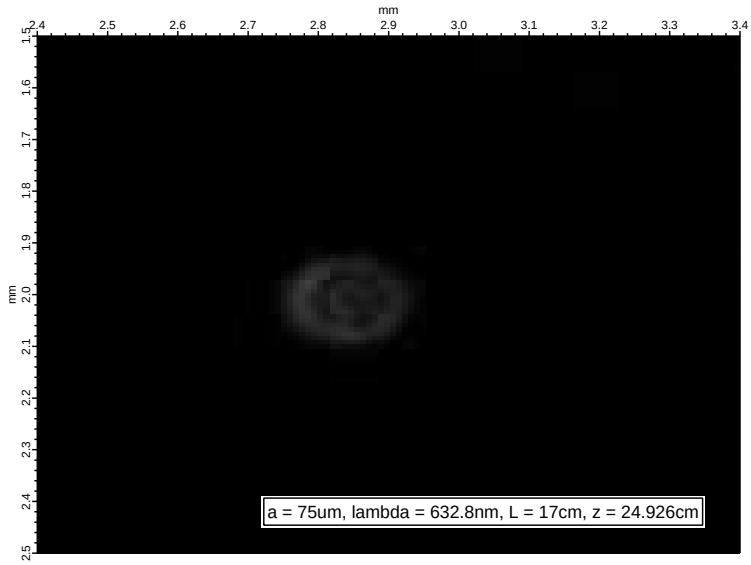

Figure 42: Projected diffraction pattern using 100 mm lens.

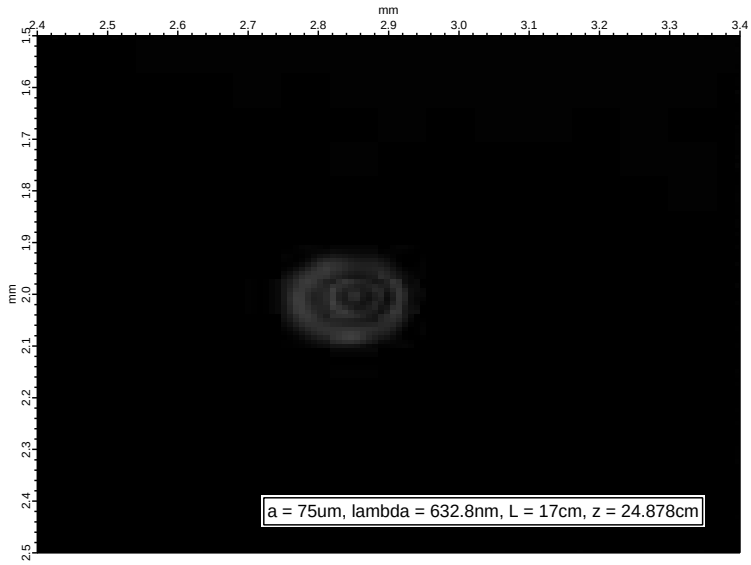

Figure 43: Projected diffraction pattern using 100 mm lens.

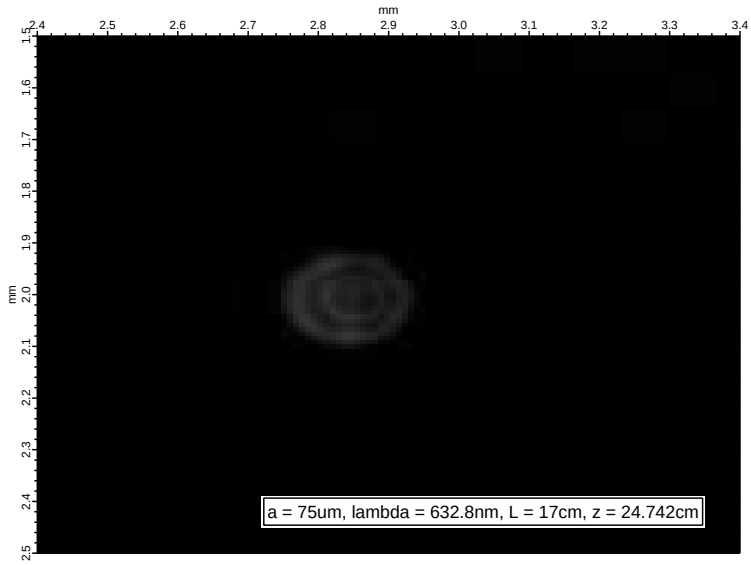

Figure 44: Projected diffraction pattern using 100 mm lens.

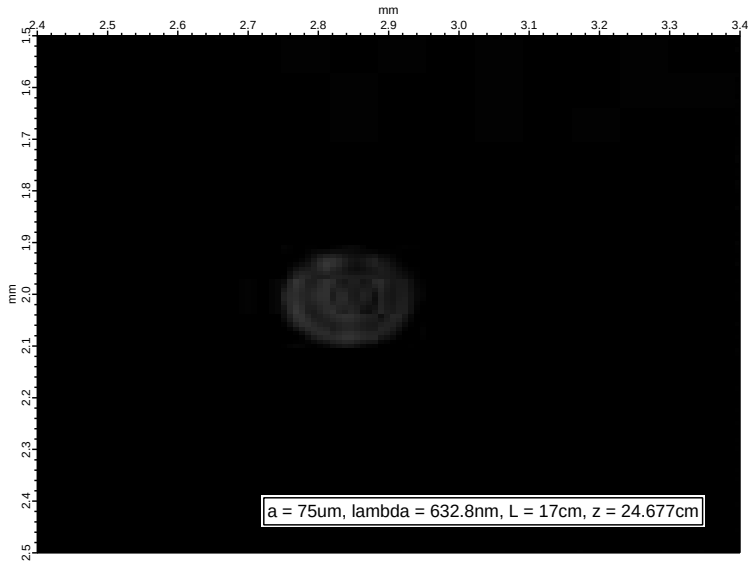

Figure 45: Projected diffraction pattern using 100 mm lens.

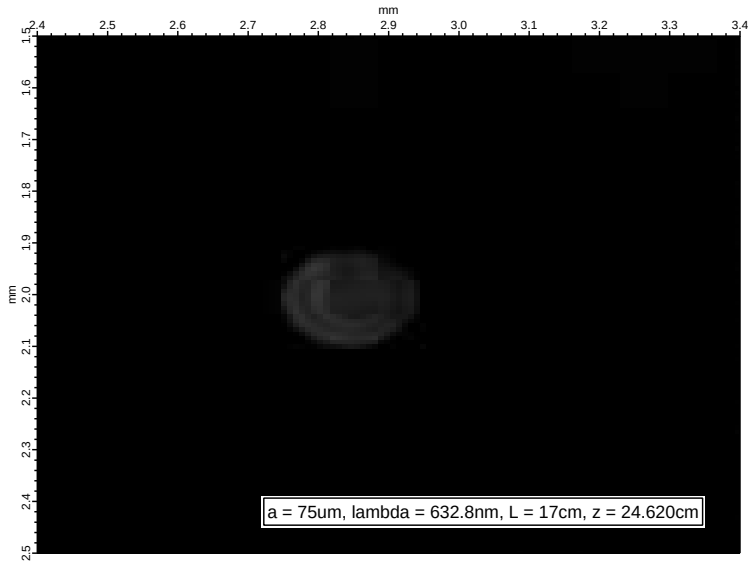

Figure 46: Projected diffraction pattern using 100 mm lens.

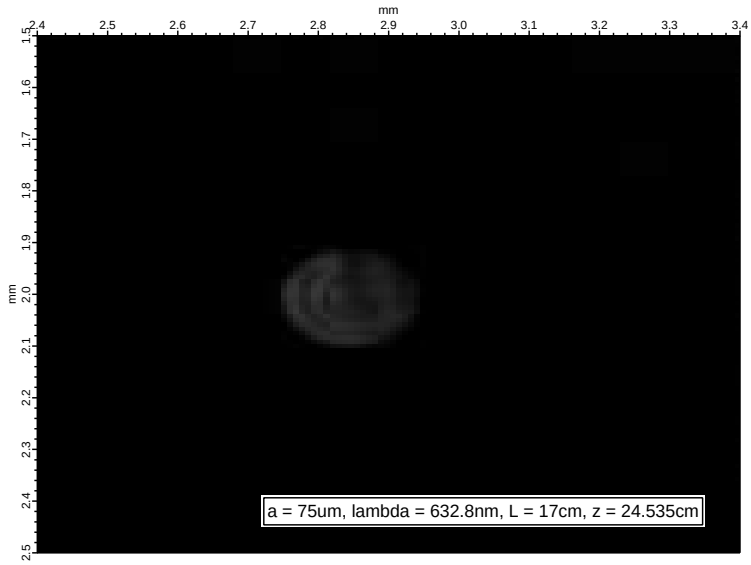

Figure 47: Projected diffraction pattern using 100 mm lens.

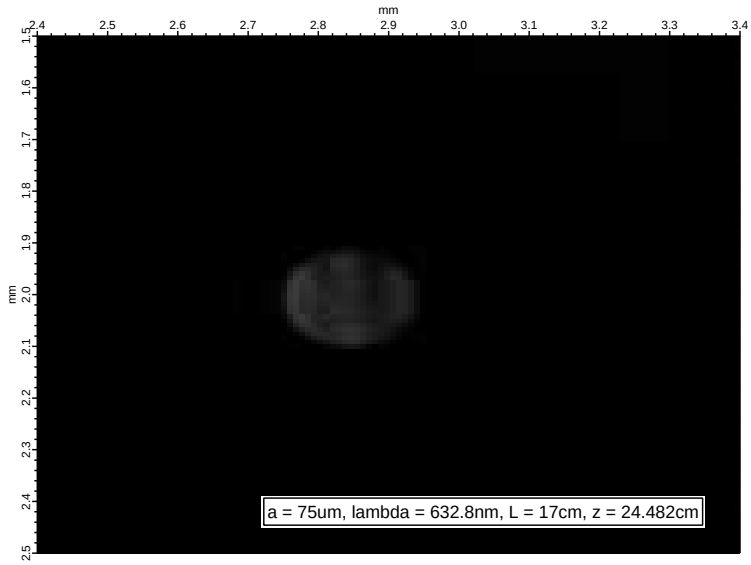

Figure 48: Projected diffraction pattern using 100 mm lens.

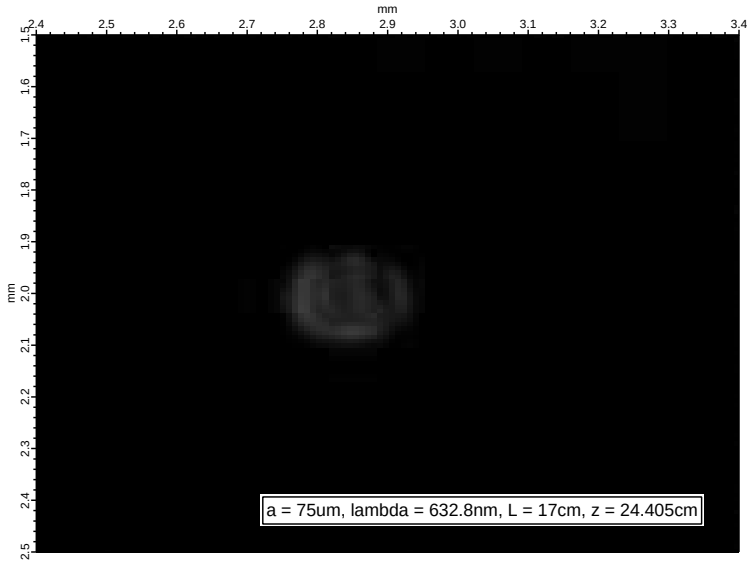

Figure 49: Projected diffraction pattern using 100 mm lens.